

Electronic Supplementary Information

Speciation of Cr(III) in intermediate phases during the sol-gel processing of Cr-doped SrTiO₃ powders

Keith A. Lehuta and Kevin R. Kittilstved*

Department of Chemistry, University of Massachusetts, Amherst, MA 01003. E-mail: kittilstved@chem.umass.edu

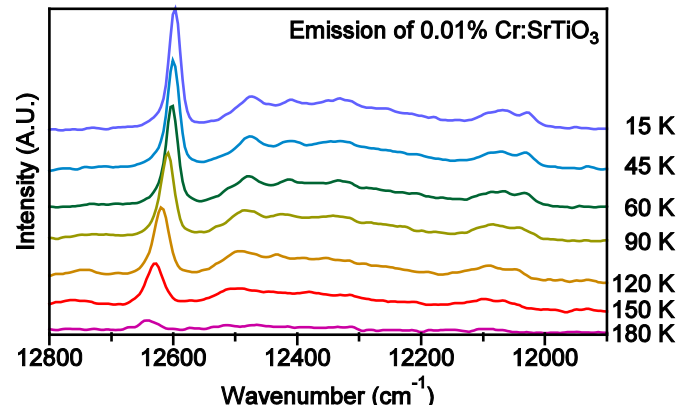


Fig. S1: Variable temperature emission of 0.01% Cr:SrTiO₃. The sample was excited by the 488 nm line of an Ar⁺ laser.

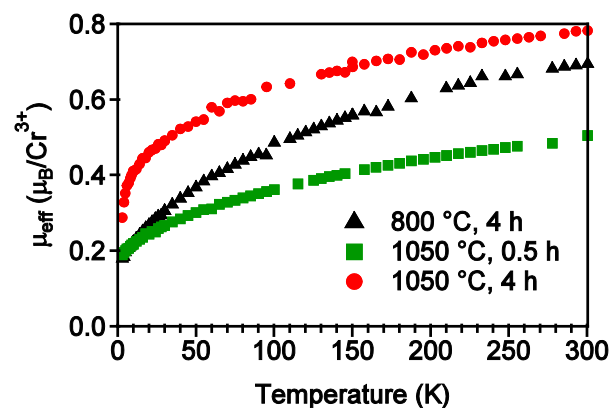


Fig. S2: Temperature dependence of the effective magnetic moment of Cr³⁺:SrTiO₃ after being annealed for 0 h (triangle), 0.5 h (square), or 4 h (circle) at 1050 °C. Effective moments are reported using the nominal Cr³⁺ concentration. Magnetic susceptibility was measured from 2-300 K on samples in an applied magnetic field of $H = 0.5$ Tesla (Quantum Design MPMS XL). Diamagnetic corrections for the SrTiO₃ host, the gel capsule¹ and kapton tape² were tabulated using reported diamagnetic susceptibilities and Pascal's tables.³

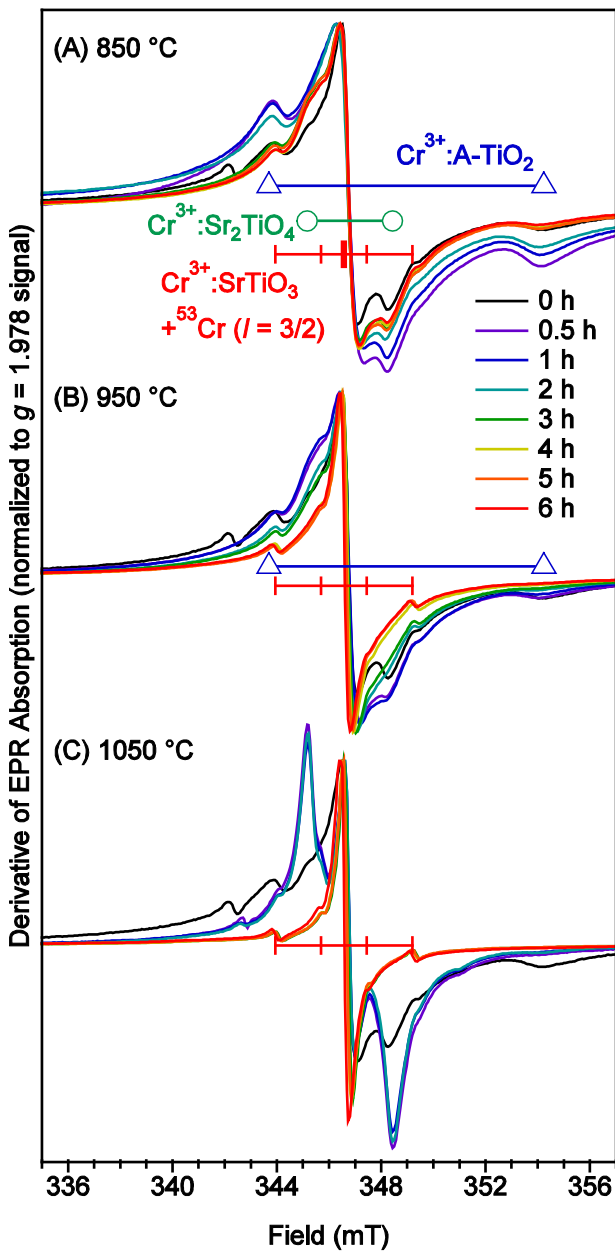


Fig. S3: Normalized EPR spectra after annealing at 850 °C (A), 950 °C (B), and 1050 °C (C). All spectra were normalized to a peak height of 1 for the Cr^{3+} feature at $g=1.978$.

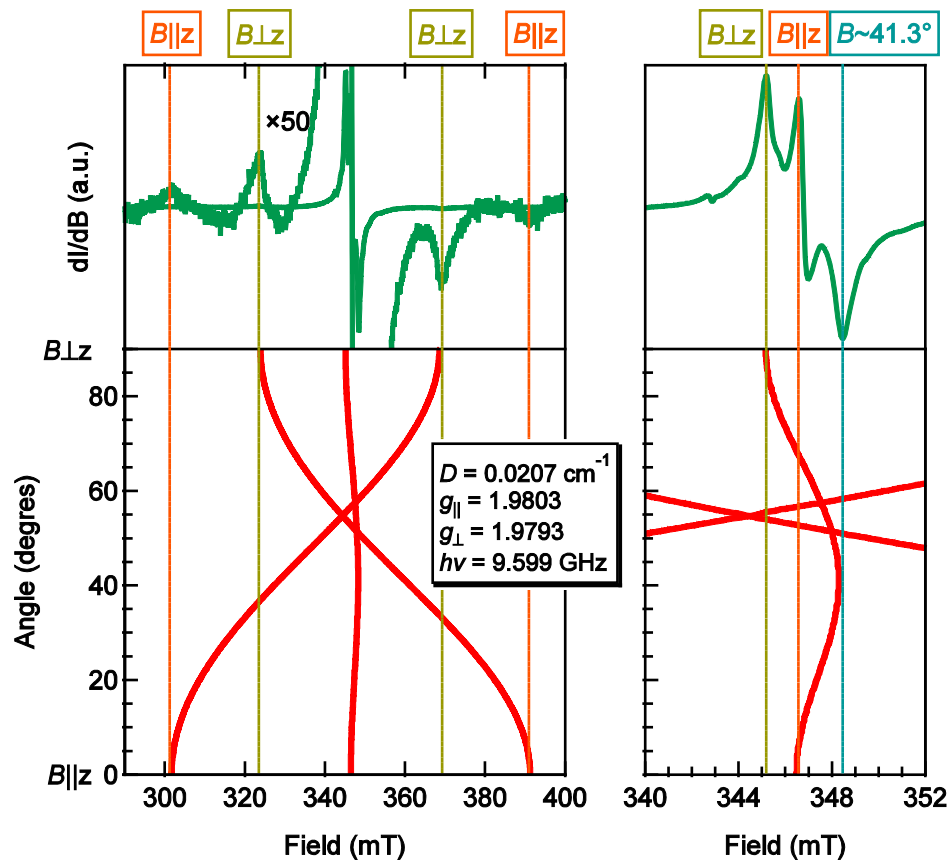


Fig. S4: Experimental EPR spectrum of polycrystalline powders of Cr-doped Sr_2TiO_4 (top) and angular dependence of the simulated EPR spectrum (bottom) with the best agreement between the EPR spectrum and the simulation. The right side of the figure shows the central features on an expanded scale. Spin-Hamiltonian parameters given in textbox. Angular dependence of the resonance fields was calculated using XSophe simulation software (Bruker Biospin).

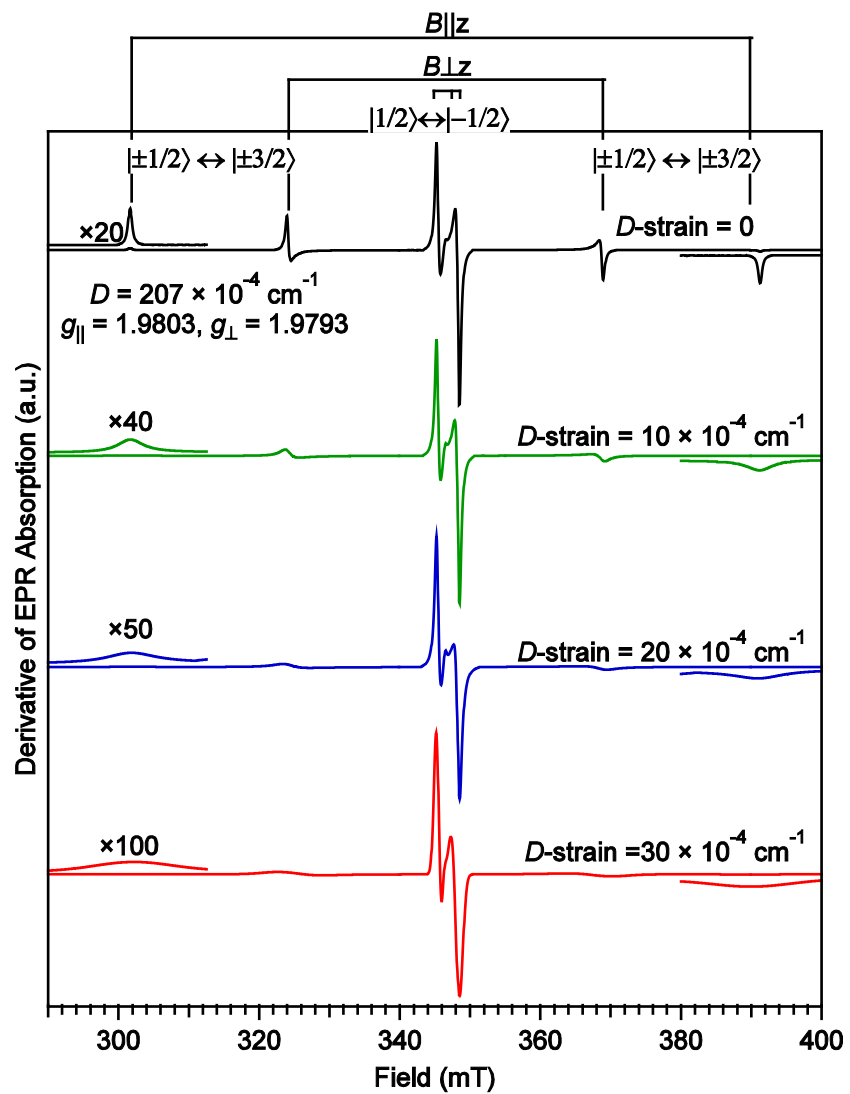


Fig. S5: Simulated EPR spectrum of $\text{Cr}^{3+}:\text{Sr}_2\text{TiO}_4$ with varying amount of D -strain from $\sigma D = 0$ (top) – $30 \times 10^{-4} \text{ cm}^{-1}$ (bottom).

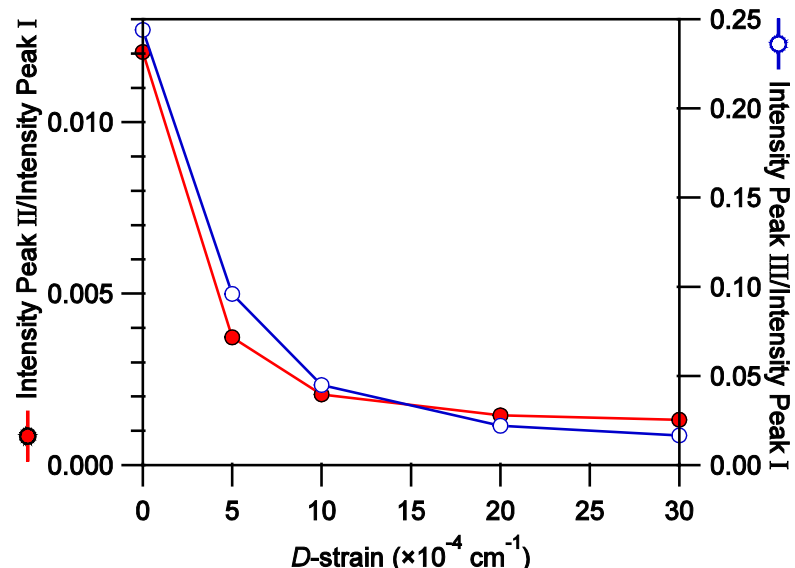


Fig. S6: EPR intensity ratio of Peak II ($|\pm 3/2\rangle \leftrightarrow |\pm 1/2\rangle$ when $B \perp z$, filled-circles) and Peak III ($|\pm 3/2\rangle \leftrightarrow |\pm 1/2\rangle$ when $B \parallel z$, open circles) to the central peak (Peak I: $|1/2\rangle \leftrightarrow |-1/2\rangle$). The intensities of the signals was taken as the peak-to-peak difference. The intensities of the $|\pm 3/2\rangle \leftrightarrow |\pm 1/2\rangle$ transitions decrease considerably compared to the central $|1/2\rangle \leftrightarrow |-1/2\rangle$ transition with small increases in the D -strain ($D = 207 \times 10^{-4} \text{ cm}^{-1}$).

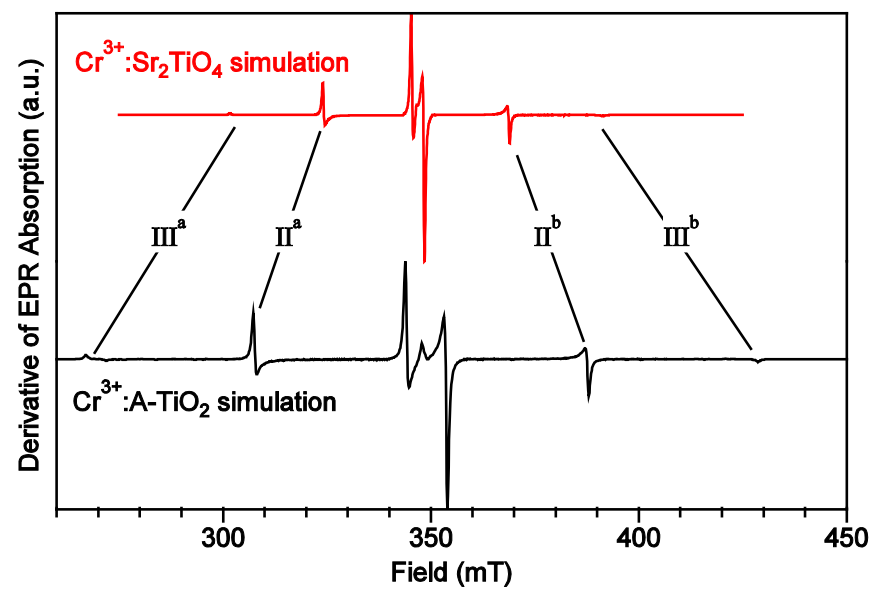


Fig. S7: Simulated EPR spectra of Cr^{3+} in the Sr_2TiO_4 phase (top) and $\text{A}-\text{TiO}_2$ phase (bottom). Input values for the simulation are given in Table 2 of the main text.

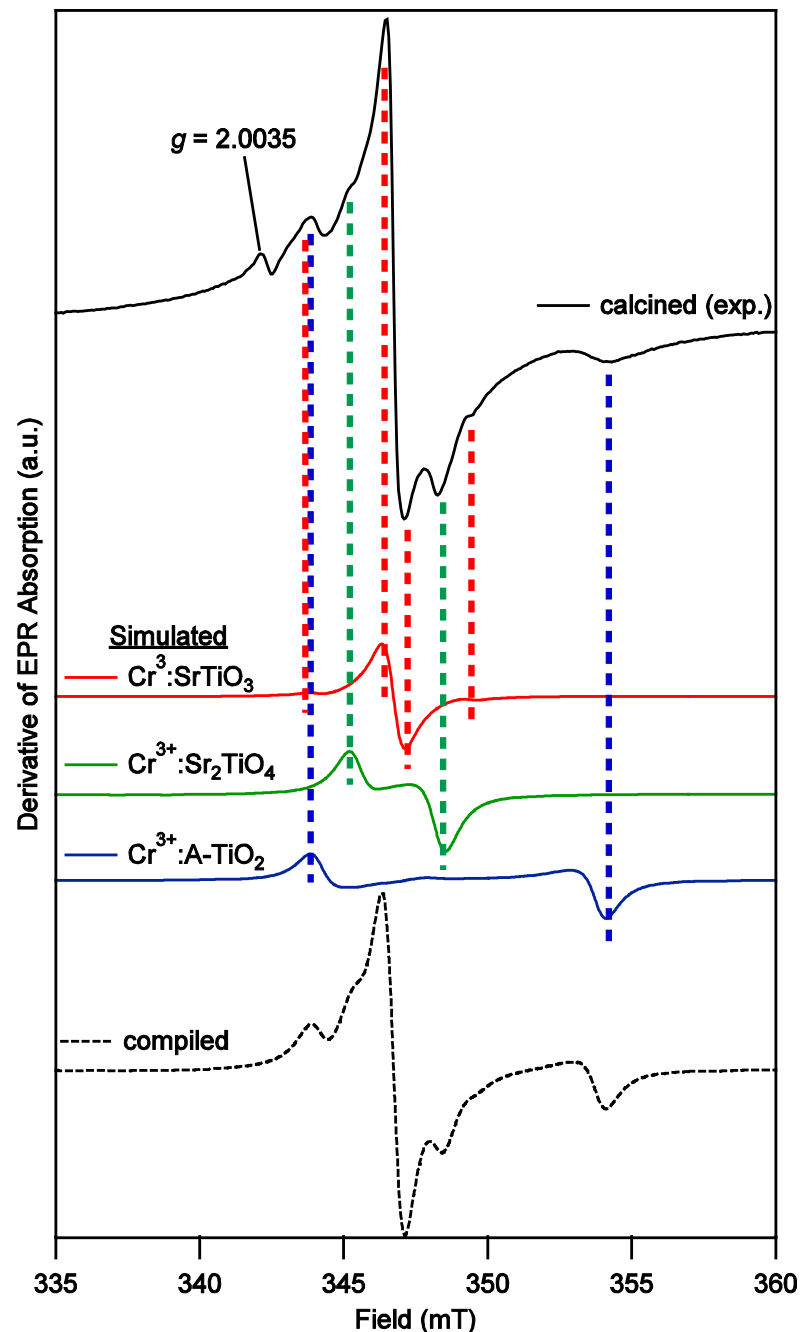


Fig. S8: Experimental EPR spectrum of calcined powders (air, 800 °C, 4 h) and simulated spectra of $\text{Cr}^{3+}:\text{SrTiO}_3$, $\text{Cr}^{3+}:\text{Sr}_2\text{TiO}_4$, and $\text{Cr}^{3+}:\text{A-TiO}_2$. The feature at $g = 2.0035$ is not due to any known Cr^{3+} phase. It is tentatively attributed to a defect in A-TiO_2 or SrTiO_3 that is rapidly oxidized > 850 °C (see Fig. S3).

ESI References

1. P. L. W. Tregenna-Piggott, *MagProp (part of the NIST DAVE software suite)*, v2.0 (20 Oct 2008), (<http://www.ncnr.nist.gov/dave>).
2. M. A. Garcia, E. Fernandez Pinel, J. de la Venta, A. Quesada, V. Bouzas, J. F. Fernández, J. J. Romero, M. S. Martín González and J. L. Costa-Krämer, *J. Appl. Phys.*, 2009, **105**, 013925.
3. G. A. Bain and J. F. Berry, *J. Chem. Ed.*, 2008, **85**, 532.